Acta Mathematicae Applicatae Sinica, English Series
Vol. 29, No. 2 (2013) 355–376
DOI: 10.1007/s10255-013-0221-7
http://www.ApplMath.com.cn & www.SpringerLink.com

Acta Mathematicae Applicatae Sinica, English Series

Complex Dynamics in a Discrete-time Predator-prey System without Allee Effect

Xian-wei CHEN[1,2], Xiang-ling FU[1], ZHU-JUN JING[2,3†]

[1]School of Mathematics and Computational Science, Hunan University of Science and Technology, Xiangtan 411201, China

[2]Department of Mathematics, Hunan Normal University, Changsha 410081, China
(E-mail: chenxianwei11@yahoo.com.cn)

[3]Academy of Mathematics and Systems Science, Chinese Academy of Sciences, Beijing 100190, China
(E-mail: jingzj@math.ac.cn)

Abstract In this paper, complex dynamics of the discrete-time predator-prey system without Allee effect are investigated in detail. Conditions of the existence for flip bifurcation and Hopf bifurcation are derived by using center manifold theorem and bifurcation theory and checked up by numerical simulations. Chaos, in the sense of Marotto, is also proved by both analytical and numerical methods. Numerical simulations included bifurcation diagrams, Lyapunov exponents, phase portraits, fractal dimensions display new and richer dynamics behaviors. More specifically, this paper presents the finding of period-one orbit, period-three orbits, and chaos in the sense of Marotto, complete period-doubling bifurcation and invariant circle leading to chaos with a great abundance period-windows, simultaneous occurrance of two different routes (invariant circle and inverse period-doubling bifurcation, and period-doubling bifurcation and inverse period-doubling bifurcation) to chaos for a given bifurcation parameter, period doubling bifurcation with period-three orbits to chaos, suddenly appearing or disappearing chaos, different kind of interior crisis, nice chaotic attractors, coexisting (2,3,4) chaotic sets, non-attracting chaotic set, and so on, in the discrete-time predator-prey system. Combining the existing results in the current literature with the new results reported in this paper, a more complete understanding is given of the discrete-time predator-prey systems with Allee effect and without Allee effect.

Keywords predator-prey system; flip bifurcation; Hopf bifurcation; Marotto's chaos; transient chaos
2000 MR Subject Classification 37N25; 65P20; 65P30

1 Introduction

In this paper, we consider the following discrete-time predator-prey system in [2]

$$F : \begin{pmatrix} x \\ y \end{pmatrix} \longrightarrow \begin{pmatrix} x + rx(1-x) - axy \\ y + ay(x-y) \end{pmatrix}, \tag{1}$$

where r and a are positive constants, x and y can be interpreted as the densities of prey and predator populations at time t, respectively. Here, $x + rx(1-x)$ stands for the rate of the increase of the prey population in the absence of predator, while the term axy represents the rate of decrease due to predation, where the parameter a is the predation parameter, the term $y + ay(x-y)$ stands for the variation of predator density with respect to the prey population.

In the following, we call the system (1) as map (1).

Manuscript received March 6, 2011.
Supported by the National Natural Science Foundation of China (No. 11071066).
†Corresponding author.

In the last few decades, the dynamics of predator-prey systems of various types have been extensively investigated and developed by many researchers. In [4, 9, 10, 14], authors studied the Holling type (Ⅱ) prey-predator system with partial-dependent and with state feedback control by using both theoretical and numerical ways, and gave the sufficient conditions for the existence of limit cycle, stability of semi-trivial and positive periodic solution, and shown that the positive periodic solution bifurcates from the semi-trivial solution through a fold bifurcation. The predator-prey models with age-structure for predator are investigated in [15], where they reported the dynamical complexities included quesiperiodic attractors and strange attractors by using numerical analysis. The dynamics of discrete-time predator-prey systems are also investigated in [7, 11, 15], where they gave the conditions of existence for flip bifurcation, Hopf bifurcation by using center manifold theorem and bifurcation theory, and provided complex dynamical behaviors by using numerical simulations. In [13] the author uses simulated data from a simple host-parasitoid model to investigate the interaction of nonlinear dynamics, noise and system identification, and to make a more "true" host-parasitoid model. The dynamical behaviors including the periodic solutions, bifurcations, chaos for the predator-prey systems with delays are also reported in [5, 6, 18, 20–27]. Fan et al[7] proved the existence of periodic solutions of nonautonomous discrete predator-prey system. Especially, the population dynamics with Allee effect have been studied. For examples, Celik et al[2] and Chen et al[3] provided the conditions of existence for stability, flip bifurcation, Hopf bifurcation, and Marotto's chaos and found richer dynamics by using both theoretical and numerical analysis.

For the map (1), Celik et al[2] obtained the local stability conditions of the equilibrium points. So, our main motivation in this paper is to investigate further the map (1) in detail.

In this paper, we give conditions on the existence of flip bifurcation and Hopf bifurcation by using bifurcation theory and center manifold Theorem[8,24], and the existence of chaos in the sense of Marotto[16,17] are proved by using both analytical and numerical methods. Numerical simulations are shown, including bifurcation diagrams, phase portraits, maximum lyapunov exponents and fractal dimension[1,12], to verify the theoretical analysis and display new and interesting dynamical behaviors of the system (1). More specifically, this paper presents the finding of period-one orbit, period-three orbits, and chaos in the sense of Marotto, complete period-doubling bifurcation and invariant circle leading to chaos with a great abundance period-windows, simultaneous occurrence of two different routs (invariant circle and inverse period-doubling bifurcation, and period-doubling bifurcation and inverse period-doubling bifurcation) to chaos for a given bifurcation parameter, period doubling bifurcation with period-three orbits to chaos, suddenly appearing or disappearing chaos, different kind of interior crisis, nice chaotic attractors, coexisting (2, 3, 4) chaotic sets, non-attracting chaotic sets, in the system (1).

By analyzing both discrete-time predator-prey systems with Allee effect[2,3] and without Allee effect (see [2] and reported in this paper), we found similar dynamical characters for the cases with or without Allee effect, such as Hopf bifurcation, flip bifurcation, Marotto's chaos, transient chaos, and different conditions of existences for various dynamical characters and the important role played by the Allee constant[2,3], Thus, a more complete understanding of the discrete-time predator-prey system (1) is given.

This paper is organized as follows: In section 2, we give the existence and stability of fixed points. In section 3, conditions on the existence of codimension-one bifurcations, including flip bifurcation and Hopf bifurcations are obtained. In section 4, conditions on the existence of Marotto's chaos are given. In section 5, numerical simulation results are presented for supporting the theoretical analysis and exhibiting new and rich dynamical behaviors.

2 Existence and Stability of Fixed Points

The fixed points of map (1) satisfy the following equations

$$\begin{cases} rx(1-x) - axy = 0, \\ ay(x-y) = 0. \end{cases}$$

By a simple analysis, it is easy to obtain the following Proposition.

Proposition 1. *For any positive parameters, the map (1) has three fixed points at* $z_1(0,0)$, $z_2(1,0)$ *and* $z_3(x^*, y^*)$, *where* $x^* = y^* = \frac{r}{a+r}$.

We now discuss the stability of the fixed points $z(x,y)$ of map (1). The Jacobian matrix J of map (1) evaluated at the fixed point $z(x,y)$ is given by

$$J = \begin{pmatrix} 1 + r - 2rx - ay & -ax \\ ay & 1 + ax - 2ay \end{pmatrix}.$$

The characteristic equation of Jacobian matrix J can be written as

$$\lambda^2 + p\lambda + q = 0, \tag{2}$$

where

$$p = -2 - r + 2rx - ax + 3ay, \qquad q = (1 + r - 2rx - ay)(1 + ax - 2ay) + a^2xy.$$

The stability of fixed points was given by Canan Celik in [2], which is stated in the following Proposition.

Proposition 2[2]**.** *The positive equilibrium point* $z_3(x^*, y^*)$ *of the predator-prey system (1) is asymptotically stable if*

$$2 - \frac{4}{r} < \frac{ar}{a+r} < 1. \tag{3}$$

3 Codimension-one Bifurcations

In this section, we give conditions on the existence of flip and Hopf bifurcations. The original system (1) undergoing fold bifurcation requires $r = -a$, which contradicts to the conditions $r > 0$ and $a > 0$. Hence the system (1) does not undergo fold bifurcation. We choose parameter a as a bifurcation parameter to study the flip bifurcation and Hopf bifurcation of the positive fixed point $z_0(x_0, y_0)$.

3.1 Flip Bifurcation

The characteristic equation associated with the linearized map (1) at $z_0(x_0, y_0)$ is given by

$$\lambda^2 + p(a)\lambda + q(a) = 0, \tag{4}$$

where

$$p(a) = -2 + r, \qquad q(a) = \Big(1 + r - \frac{2r^2 + ar}{a+r}\Big)\Big(1 - \frac{ar}{a+r}\Big) + \frac{a^2r^2}{a+r}.$$

Let

$$a_0 = \frac{2r(r-2)}{r^2 - 2r + 4}. \tag{5}$$

Then the eigenvalues of the fixed point $z_0(x_0(a_0), y_0(a_0))$ are

$$\lambda_1 = -1, \qquad \lambda_2 = 3 - r.$$

We require $|\lambda_2| \neq 1$. This leads to the fact that $p(r_0) \neq 0, 2$. So we get

$$r \neq 2 \qquad \text{and} \qquad r \neq 4. \tag{6}$$

Let $w = x - x_0,\ v = y - y_0$ and $\overline{a} = a - a_0$. We transform the fixed point $z_0(x_0, y_0)$ to the origin and consider the parameter $\overline{a}$ as a new dependent variable. Thus, map (1) becomes

$$\begin{pmatrix} w \\ \overline{a} \\ v \end{pmatrix} \longrightarrow \begin{pmatrix} a_{11} & a_{12} & a_{13} \\ 0 & -1 & 0 \\ a_{31} & 0 & a_{33} \end{pmatrix} \begin{pmatrix} w \\ \overline{a} \\ v \end{pmatrix} + \begin{pmatrix} f_1(w, \overline{a}, v) \\ 0 \\ f_2(w, \overline{a}, v) \end{pmatrix}, \tag{7}$$

where

$$\begin{aligned}
a_{11} &= \frac{3r - r^2 - 4}{r}, \\
a_{12} &= -\frac{(r^2 - 2r + 4)^2}{r^4}, \\
a_{13} &= \frac{-2r + 4}{r}, \\
a_{31} &= \frac{2r - 4}{r}, \\
a_{33} &= \frac{-r + 4}{r}, \\
f_1(w, \overline{a}, v) &= -rw^2 - x_0\bar{a}v - a_0wv - y_0\bar{a}w - \bar{a}wv, \\
f_2(w, \overline{a}, v) &= -a_0v^2 + a_0wv - 2y_0\bar{a}v + y_0\bar{a}w - \bar{a}v^2 + x_0\bar{a}v + \bar{a}wv.
\end{aligned}$$

Let $n = \frac{r^4(r-4)}{(r^2-2r+4)^2}$, we construct an invertible matrix

$$T = \begin{pmatrix} a_{33} + 1 & -1 & a_{33} - \lambda_2 \\ 0 & n & 0 \\ -a_{31} & 0 & -a_{31} \end{pmatrix},$$

and under the transformation

$$\begin{pmatrix} w \\ \overline{a} \\ v \end{pmatrix} = T \begin{pmatrix} X \\ \mu \\ Y \end{pmatrix},$$

the map (7) becomes

$$\begin{pmatrix} X \\ \mu \\ Y \end{pmatrix} \longrightarrow \begin{pmatrix} -1 & 1 & 0 \\ 0 & -1 & 0 \\ 0 & 0 & \lambda_2 \end{pmatrix} \begin{pmatrix} X \\ \mu \\ Y \end{pmatrix} + \begin{pmatrix} F_1(X,\ \mu,\ Y) \\ 0 \\ F_2(X,\ \mu,\ Y) \end{pmatrix}, \tag{8}$$

where

$$\begin{aligned}
F_1(X, \mu, Y) =& \frac{1}{\lambda_2 + 1}(-rw^2 - x_0\overline{a}v - a_0wv - y_0\overline{a}w - \bar{a}wv) \\
&+ \frac{a_{33} - \lambda_2}{a_{31}(1 + \lambda_2)}(-a_0v^2 + a_0wv - 2y_0\overline{a}v + y_0\overline{a}w - \overline{a}v^2 + x_0\overline{a}v + \overline{a}wv),
\end{aligned}$$

$$\begin{aligned}
F_2(X,\mu,Y) =& -\frac{1}{\lambda_2+1}(-rw^2 - x_0\overline{a}v - a_0wv - y_0\overline{a}w - \overline{a}wv)\\
&-\frac{a_{33}+1}{a_{31}(1+\lambda_2)}(-a_0v^2 + a_0wv - 2y_0\overline{a}v + y_0\overline{a}w - \overline{a}v^2 + x_0\overline{a}v + \overline{a}wv),\\
w =&(a_{33}+1)X - \mu - (a_{33}-\lambda_2)Y,\\
\overline{a} =&n\mu,\\
v =&-a_{31}X - a_{31}Y.
\end{aligned}$$

By the center manifold theorem, the stability of $(X,Y)=(0,0)$ near $\mu=0$ can be determined by studying a one-parameter family of maps on a center manifold, which can be written as:

$$W^c(0)=\big\{(X,\mu,Y)\in R^3 \mid Y=h^*(X,\mu),\ h^*(0,0)=0,\ Dh^*(0,0)=0\big\}.$$

Assume a center manifold with

$$h^*(X,\ \mu)=m_1X^2+m_2X\mu+m_3\mu^2+\mathrm{O}(3), \tag{9}$$

where O(3) is the sum of all terms whose order is great than 2.

Then the center manifold must satisfy

$$N(h^*(X,\mu))=h^*(-X+\mu+F_1(X,\mu,h^*(X,\mu)),\mu)-\lambda_2h^*(X,\mu)-F_2(X,\mu,h^*(X,\mu))=0. \tag{10}$$

Substituting (8) and (9) into (10) and comparing coefficients of Eq. (10), one obtains

$$\begin{aligned}
m_1 &= \frac{-16r}{(r^2-2r+4)(r-4)(r-2)},\\
m_2 &= \frac{2r(r^3-6r^2+24r-56)}{(r^2-2r+4)(r-2)(r-4)^2},\\
m_3 &= \frac{-2r(3r^2-12r+4)}{(r-4)^2(r^2-2r+4)(r-2)}.
\end{aligned}$$

Thus the map restricted to the center manifold is given by

$$\begin{aligned}
F^*: X \longrightarrow & -X+\mu+h_1X^2+h_2X\mu+h_3\mu^2+h_4m_1X^3+(h_4m_2+h_5m_1+h_7)X^2\mu\\
&+(h_4m_3+h_5m_2+h_6)X\mu^2+h_5m_3\mu^3+\mathrm{O}((|X|+|\mu|)^4),
\end{aligned} \tag{11}$$

where

$$\begin{aligned}
h_1 =&\frac{4r(r^2-6r+12)}{(r^2-2r+4)(r-4)},\\
h_2 =&-\frac{r(r^3-2r^2-16r+56)}{(r-4)(r^2-2r+4)},\\
h_3 =&\frac{r(r^3-6r^2-12r+8)}{2(r-4)(r^2-2r+4)},\\
h_4 =&-\frac{2(r+4)(r^2-4r+8)(r-2)^2}{r(r^2-2r+4)(r-4)},\\
h_5 =&\frac{(r-2)(r^4-8r^3+20r^2+24r-64)}{2(r-4)(r^2-2r+4)},\\
h_6 =&-\frac{r^3(r-2)(r-4)}{(r^2-2r+4)^2},\\
h_7 =&\frac{2r^2(r^4-8r^3+16r^2+8r-32)}{(r-4)(r^2-2r+4)^2}.
\end{aligned}$$

In order for map (11) to undergo a flip bifurcation, it is also required that

$$\alpha_1 = \Big[\frac{\partial F^*}{\partial \mu}\cdot\frac{\partial^2 F^*}{\partial X^2} + 2\frac{\partial^2 F^*}{\partial X \partial \mu}\Big]\Big|_{(0,0)} \neq 0$$

and

$$\alpha_2 = \Big[\frac{1}{2}\cdot(\frac{\partial^2 F^*}{\partial X^2})^2 + \frac{1}{3}\cdot\frac{\partial^3 F^*}{\partial X^3}\Big]\Big|_{(0,0)} \neq 0.$$

It is obvious that

$$\alpha_1 = -\frac{2r(r^3-6r^2+8r+8)}{(r-4)(r^2-2r+4)} \neq 0,$$
$$\alpha_2 = \frac{32(r^6-12r^5+62r^4-148r^3+128r^2+96r-128)}{(r-4)^2(r^2-2r+4)^2} \neq 0.$$

From the above analysis, we have the following theorem.

Theorem 1. *The map (1) undergoes a flip bifurcation at $z(x_0(a_0), y_0(a_0))$ if (5), (6) and the following conditions are satisfied:*

$$\alpha_1 \neq 0 \qquad \textit{and} \qquad \alpha_2 \neq 0.$$

Moreover, if $\alpha_2 > 0$ (< 0), the period-2 points that bifurcate from this fixed point are stable (resp. unstable).

3.2 Hopf Bifurcation

Next, a condition of the existence of Hopf bifurcation of map (1) is derived by using the Hopf bifurcation theorem [7, 24].

The characteristic equation associated with the linearizated map (1) at the fixed point $z(x_0(a), y_0(a))$ is given by

$$\lambda^2 + p(a)\lambda + q(a) = 0. \tag{12}$$

The eigenvalues of the characteristic equation (12) are given as

$$\lambda_{1,2}(a) = \frac{-p(a) \pm \sqrt{p^2(a) - 4q(a)}}{2}, \tag{13}$$

where

$$p(a) = -2 - r + 2rx_0 - ax_0 + 3ay_0,$$
$$q(a) = (1 + r - 2rx_0 - ay_0)(1 + ax_0 - 2ay_0) + a^2 x_0 y_0.$$

The eigenvalues $\lambda_{1,2}(a)$ are complex conjugate for $p^2(a) - 4q(a) < 0$, which leads to

$$(r - 2rx_0 - ax_0 + ay_0)^2 < 4a^2 x_0 y_0. \tag{14}$$

According to inequality (14) and $(x_0, y_0) = \big(\frac{r}{r+a}, \frac{r}{r+a}\big)$, we obtain

$$0 < r < 3a. \tag{15}$$

Let

$$\overline{a} = \frac{r}{r-1}, \qquad \text{for } r \neq 1. \tag{16}$$

We get that $q(\overline{a})=1$ and $\lambda_{1,2}(\overline{a})=\frac{2-r}{2}\pm\frac{i\sqrt{4r-r^2}}{2}=\alpha_1\pm i\alpha_2$.

Under the conditions (15) and (16), we have

$$|\lambda_{1,2}(a)|=(q(a))^{\frac{1}{2}}\qquad\text{and}\qquad d=\frac{d|\lambda_{1,2}(a)|}{da}\Big|_{a=\overline{a}}=\frac{r^2}{2(r+\overline{a})}\neq 0. \tag{17}$$

In addition, if $p(\overline{a})\neq 0,1$, which leads to

$$\overline{a}\neq 2\qquad\text{and}\qquad \overline{a}\neq\frac{2r}{1+r}, \tag{18}$$

then we obtain that $\lambda_{1,2}^n(\overline{a})\neq 1$ $(n=1,2,3,4)$.

Let $\begin{cases} w=x-x_0,\\ v=y-y_0.\end{cases}$ The map (1) becomes

$$G:\begin{pmatrix} w\\ v\end{pmatrix}\longrightarrow\begin{pmatrix} r-2rx_0 & -1\\ 1 & 0\end{pmatrix}\begin{pmatrix} w\\ v\end{pmatrix}+\begin{pmatrix} f_1(w,v)\\ f_2(w,v)\end{pmatrix}, \tag{19}$$

where

$$f_1(w,v)=-rw^2-\overline{a}wv,\qquad f_2(w,v)=\overline{a}wv-\overline{a}v^2.$$

Using the transformation $\begin{pmatrix} w\\ v\end{pmatrix}=T\begin{pmatrix} X\\ Y\end{pmatrix}$, where $T=\begin{pmatrix} -1 & 0\\ \alpha_1-r+2rx_0 & -\alpha_2\end{pmatrix}$, then map (19) becomes

$$\begin{pmatrix} X\\ Y\end{pmatrix}\longrightarrow\begin{pmatrix} \alpha_1 & -\alpha_2\\ \alpha_2 & \alpha_1\end{pmatrix}\begin{pmatrix} X\\ Y\end{pmatrix}+\begin{pmatrix} F_1(X,Y)\\ F_2(X,Y)\end{pmatrix}, \tag{20}$$

where

$$\begin{aligned}
F_1(X,Y)=&rX^2-\overline{a}(\alpha_1-r+2rx_0)X^2+\overline{a}\alpha_2XY,\\
F_2(X,Y)=&\frac{\alpha_1-r+2rx_0}{\alpha_2}[rX^2-\overline{a}(\alpha_1-r+2rx_0)X^2+\overline{a}\alpha_2XY]\\
&+\frac{1}{\alpha_2}[\overline{a}(\alpha_1-r+2rx_0)+\overline{a}(\alpha_1-r+2rx_0)^2]X^2+\overline{a}\alpha_2Y^2\\
&-[\overline{a}+2\overline{a}(\alpha_1-r+2rx_0)]XY.
\end{aligned}$$

Next, we study the Hopf bifurcation of map (20) using the method given in [7]. The coefficients are given as follows:

$$\begin{aligned}
l_1=&-\mathrm{Re}\Big[\frac{(1-2\lambda)\overline{\lambda}^2}{1-\lambda}\xi_{11}\xi_{20}\Big]-\frac{1}{2}|\xi_{11}|^2-|\xi_{02}|^2+\mathrm{Re}\,(\overline{\lambda}\xi_{21}),\\
\xi_{20}=&\frac{1}{8}[(F_{1XX}-F_{1YY}+2F_{2XY})+i(F_{2XX}-F_{2YY}-2F_{1XY})],\\
\xi_{11}=&\frac{1}{4}[(F_{1XX}+F_{1YY})+i(F_{2XX}+F_{2YY})],\\
\xi_{02}=&\frac{1}{8}[(F_{1XX}-F_{1YY}-2F_{2XY})+i(F_{2XX}-F_{2YY}+2F_{1XY})],\\
\xi_{21}=&\frac{1}{16}[(F_{1XXX}+F_{1XYY}+F_{2XXY}+F_{2YYY})\\
&+i\big(F_{2XXX}+F_{2XYY}-F_{1XXY}-F_{1YYY}\big)\big].
\end{aligned}$$

Thus, some complicated calculation gives

$$\begin{aligned} l_1 = &- \frac{1}{32((1-\alpha_1)^2+\alpha_2^2)}\big\{M[F_{1XX}(F_{1XX}+2F_{2XY})-(F_{2XX}-F_{2YY}-2F_{1XY}) \\ &\times (F_{2XX}+F_{2YY})]+N[2F_{1XX}(F_{2XX}-F_{1XY})+2F_{2XY}(F_{2XX}+F_{2YY})]\big\} \\ &- \frac{1}{32}\big[F_{1XX}^2+(F_{2XX}+F_{2YY})^2\big] \\ &- \frac{1}{64}\big[(F_{1XX}-2F_{2XY})^2+(F_{2XX}-F_{2YY}+2F_{1XY})^2\big], \end{aligned} \tag{21}$$

where

$$\begin{aligned} &F_{1XX} = 2[r^2-\overline{a}(\alpha_1-r+2rx_1)], \\ &F_{1XY} = \overline{a}\alpha_2, \\ &F_{2XX} = \frac{2(\alpha_1-r-2rx_1)(r+\overline{a})}{\alpha_2}, \\ &F_{2XY} = -\overline{a}(1+\alpha_1-r+2rx_1), \\ &F_{2YY} = 2\overline{a}\alpha_2, \\ &M = \alpha_1^2-3\alpha_1^3+2\alpha_1^4-\alpha_2^2+\alpha_1\alpha_2^2-2\alpha_2^4, \\ &N = -\alpha_2(\alpha_2^2+5\alpha_1^2-2\alpha_1-4\alpha_1^3-4\alpha_1\alpha_2^2), \\ &\alpha_1 = \frac{2-r}{2}, \\ &\alpha_2 = \frac{\sqrt{4r-r^2}}{2}. \end{aligned}$$

From the above analysis, we have the following theorem.

Theorem 2. *The map (1) undergoes a Hopf bifurcation at the fixed point $z(x_0, y_0)$ if the conditions (15), (16), (18) hold and $l \neq 0$ in (21). Moreover, if $l_1 < 0$ (resp. $l_1 > 0$) and $d > 0$, then an attracting (resp. repelling) invariant closed curve bifurcates from the fixed point for $a > \overline{a}$ (resp. $a < \overline{a}$).*

4 Existence of Marotto's Chaos

In this section, we prove that the map (1) possesses a chaotic behavior in the sense of Marrotto (see 16,17]).

We first give a condition under which the fixed point $z_0(x_0, y_0)$ of map (1) is a snap-back repeller. The eigenvalues associated with the fixed point $z_0(x_0, y_0)$ are given by

$$\lambda_{1,2} = \frac{-p(x_0,y_0) \pm \sqrt{p^2(x_0,y_0)-4q(x_0,y_0)}}{2},$$

where

$$\begin{aligned} &p(x,y) = -2-r+2rx-ax+3ay, \\ &q(x,y) = (1+r-2rx-ay)(1+ax-2ay)+a^2xy. \end{aligned}$$

We need to find a neighborhood $U_r(z_0)$ of $z_0(x_0, y_0)$ in which the norm of eigenvalues exceeds 1 for all $z \in U_r(z_0)$. This is equivalent to the condition

$$\begin{cases} p^2(x,y)-4q(x,y) < 0, \\ q(x,y)-1 > 0. \end{cases}$$

Let

$$S_1(x,y) = p^2(x,y) - 4q(x,y) = a^2y^2 + (2a\beta_1 - 4a^2x)y + \beta_1^2,$$

where $\beta_1 = r - 2rx - ax$. Since

$$\triangle_1 = (2a\beta_1 - 4a^2x)^2 - 4\beta_1^2a^2 \geq 0,$$

the equation $S_1(x,y) = 0$ has one real root with multiplicity 2 or two real roots denoted as

$$\overline{y_1} = \frac{2ax - \beta_1 - \sqrt{4a^2x^2 - 4a\beta_1 x}}{a} \qquad \text{and} \qquad \overline{y_2} = \frac{2ax - \beta_1 + \sqrt{4a^2x^2 - 4a\beta_1 x}}{a}.$$

Since

$$\triangle_1 = (2a\beta_1 - 4a^2x)^2 - 4\beta_1^2a^2 \geq 0,$$

we obtain that

$$x \geq \frac{r}{2(a+r)}.$$

Thus, $S_1(x,y) < 0$ if $x \in D_1 = \left\{x | x \geq \frac{r}{2(a+r)}\right\}$ and $y \in D_3 = (\overline{y_1}, \overline{y_2})$.

Let

$$S_2(x,y) = q(x,y) - 1 = 2a^2y^2 - (a + 2\beta_2)y + r - 2rx + \beta_2 x,$$

where $\beta_2 = a + ar - 2arx$. If $\triangle_2 = (a + 2\beta_2)^2 - 8a^2(r - 2rx + \beta_2 x) \geq 0$, then the equation $S_2(x,y) = 0$ has one real root with multiplicity 2 or two real roots both denoted as

$$\overline{y_1}' = \frac{a + 2\beta_2 - \sqrt{\triangle_2}}{4a^2}, \qquad \overline{y_2}' = \frac{a + 2\beta_2 + \sqrt{\triangle_2}}{4a^2}.$$

Since $\triangle_2 \geq 0$, we obtain that

$$16a^2r(r+a)x^2 - 8a^2(2r^2 + a + ar)x + 9a^2 + 4a^2r + 4a^2r^2 \geq 0, \tag{22}$$

If $\triangle_3 = 64(a^2 + a^2r^2 + 2a^2r - 9r^2 - 4r^3 - 9ar) \geq 0$, from (22) we get that $x \geq x_1$ or $x \leq x_2$, where

$$x_1 = \frac{2r^2 + a + ar + \sqrt{\triangle_3}}{4r(r+a)}, \qquad x_2 = \frac{2r^2 + a + ar - \sqrt{\triangle_3}}{4r(r+a)}.$$

If $\triangle_3 < 0$ from (22), we obtain that $x \in R$.

If $\triangle_3 > 0$ and $x_2 < x < x_1$, then $\triangle_2 < 0$, so we have $y \in R$.

Therefore, we obtain that $S_2(x,y) > 0$ if one of the following conditions holds:

(1) $\triangle_3 \geq 0,\ x \in D_2 = (-\infty, x_2) \cup (x_1, +\infty)$ and $y \in D_3' = (-\infty,\ \overline{y_1}') \cup (\overline{y_2}', +\infty)$;

(2) $\triangle_3 < 0,\ x \in R$ and $y \in D_3'$;

(3) $\triangle_3 > 0,\ x \in D_2' = (x_2, x_1)$.

According to the above analysis, we can get the following lemma.

Lemma 1. *Let $a > 0,\ r > 0$ if one of the following conditions is satisfied:*

(i) $\triangle_3 \geq 0,\ x \in D_1 \cap D_2$ and $y \in D_3 \cap D_3'$;

(ii) $\triangle_3 < 0,\ x \in D_1$ and $y \in D_3 \cap D_3'$;

(iii) $\triangle_3 > 0,\ x \in D_1 \cap D_2'$ and $y \in D_3$.

Then $p^2(x,y) - 4q(x,y) < 0$ and $q(x,y) - 1 > 0$. Moveover, if the fixed point $z_0(x_0,y_0)$ of map (1) satisfies

$$z_0(x_0,y_0) \in U_{z_0} = \left\{(x,y) \mid x \in D_1 \cap D_2,\ y \in D_3 \cap D_3'\right\}$$

or

$$z_0(x_0,y_0) \in U_{z_0} = \left\{(x,y) \mid x \in D_1,\ y \in D_3 \cap D_3'\right\}$$

or

$$z_0(x_0, y_0) \in U_{z_0} = \big\{(x, y) \mid x \in D_1 \cap D_2',\ y \in D_3\big\},$$

then $z_0(x_0, y_0)$ *is an expanding fixed point in* U_{z_0}.

According to the definition of snap-back repeller, one needs to find one point $z_1(x_1, y_1) \in U_{z_0}$ such that $z_1 \neq z_0$, $F^M(z_1) = z_0$, and $|DF^M(z_1)| \neq 0$ for some positive integer M, where map F is defined by (1).

To proceed, notice that

$$\begin{cases} x_1 + rx_1(1 - x_1) - ax_1y_1 = x_2, \\ y_1 + ay_1(x_1 - y_1) = y_2, \end{cases} \tag{23}$$

and

$$\begin{cases} x_2 + rx_2(1 - x_2) - ax_2y_2 = x_0, \\ y_2 + ay_2(x_2 - y_2) = y_0. \end{cases} \tag{24}$$

Now, a map F^2 has been constructed to map the point $z_1(x_1, y_1)$ to the fixed point $z_0(x_0, y_0)$ after two iterations if Eqs. (23) and (24) have solutions being different from z_0. The solutions of Eq. (24) which are different from z_0, satisfy the equation

$$\begin{cases} -[x_2 - x_0 + rx_2(1 - x_2)]^2 + (x_2 + ax_2^2)[x_2 - x_0 + rx_2(1 - x_2)] - ay_0x_2^2 = 0, \\ y_2 = \dfrac{1}{ax_2}[x_2 - x_0 + rx_2(1 - x_2)]. \end{cases} \tag{25}$$

Let

$$\begin{aligned} &A = r^2 + ar, && B = -(2r^2 + r + a + ar), \\ &C = r^2 + r + 2rx_0 + ay_0 + ax_0, && D = x_0 + 2rx_0, \qquad E = x_0^2. \end{aligned}$$

From (25), one can get

$$Ax_2^4 + Bx_2^3 + Cx_2^2 + Dx_2 + E = 0. \tag{26}$$

Let

$$\begin{aligned} \alpha &= -\frac{3B^2}{8A^2} + \frac{C}{A}, \\ \beta &= \frac{B^3}{8A^3} - \frac{BC}{2A^2} + \frac{D}{A}, \\ \gamma &= -\frac{3B^4}{256A^4} + \frac{B^2C}{16A^3} - \frac{BD}{4A^2} + \frac{E}{A}, \\ P &= -\frac{\alpha^2}{12} - \gamma, \\ Q &= -\frac{\alpha^3}{108} + \frac{\alpha\gamma}{3} - \frac{\beta^2}{8}, \\ R &= \frac{Q}{2} \pm \sqrt{\frac{Q^2}{4} + \frac{P^3}{27}}, \\ U &= \sqrt[3]{R}, \\ \xi &= -\frac{5\alpha}{6} + \frac{P}{3U} - U. \end{aligned}$$

If $\beta = 0$ and $\alpha < -2\sqrt{r}$, then the equation (26) has four real roots denoted as

$$x_{11} = -\frac{B}{4A} + \sqrt{\frac{-\alpha + \sqrt{\alpha^2 - 4r}}{2}},$$
$$x_{12} = -\frac{B}{4A} + \sqrt{\frac{-\alpha - \sqrt{\alpha^2 - 4r}}{2}},$$
$$x_{13} = -\frac{B}{4A} - \sqrt{\frac{-\alpha + \sqrt{\alpha^2 - 4r}}{2}},$$
$$x_{14} = -\frac{B}{4A} - \sqrt{\frac{-\alpha - \sqrt{\alpha^2 - 4r}}{2}}.$$

If $\beta \neq 0$, $\alpha + 2\xi > 0$ and $3\alpha + 2\xi < \frac{2\beta}{\sqrt{2\xi+\alpha}}$ or $3\alpha + 2\xi < -\frac{2\beta}{\sqrt{2\xi+\alpha}}$, then equation (26) has real roots denoted as

$$x'_{11} = -\frac{B}{4A} + \frac{-\sqrt{\alpha + 2\xi} \pm \sqrt{-(3\alpha + 2\xi - \frac{2\beta}{\sqrt{\alpha+2\xi}})}}{2},$$

or

$$x'_{11} = -\frac{B}{4A} + \frac{\sqrt{\alpha + 2\xi} \pm \sqrt{-(3\alpha + 2\xi + \frac{2\beta}{\sqrt{\alpha+2\xi}})}}{2}.$$

Substituting x_2 and y_2 into Eqs. (23) and solving x_1, y_1, we get

$$\begin{cases} -[x_1 - x_2 + rx_1(1 - x_1)]^2 + (x_1 + ax_1^2)[x_1 - x_2 + rx_1(1 - x_1)] - ay_2x_1^2 = 0, \\ y_1 = \dfrac{1}{ax_1}[x_1 - x_2 + rx_1(1 - x_1)]. \end{cases} \tag{27}$$

Let

$$\overline{A} = r^2 + ar, \qquad \overline{B} = -(2r^2 + r + a + ar),$$
$$\overline{C} = r^2 + r + 2rx_2 + ay_2 + ax_2, \qquad \overline{D} = x_2 + 2rx_2, \qquad \overline{E} = x_2^2,$$
$$\overline{\alpha} = -\frac{3\overline{B}^2}{8\overline{A}^2} + \frac{\overline{C}}{\overline{A}},$$
$$\overline{\beta} = \frac{\overline{B}^3}{8\overline{A}^3} - \frac{\overline{BC}}{2\overline{A}^2} + \frac{\overline{D}}{\overline{A}},$$
$$\overline{\gamma} = -\frac{3\overline{B}^4}{256\overline{A}^4} + \frac{\overline{B}^2\overline{C}}{16\overline{A}^3} - \frac{\overline{BD}}{4\overline{A}^2} + \frac{\overline{E}}{\overline{A}},$$
$$\overline{P} = -\frac{\overline{\alpha}^2}{12} - \overline{\gamma},$$
$$\overline{Q} = -\frac{\overline{\alpha}^3}{108} + \frac{\overline{\alpha\gamma}}{3} - \frac{\overline{\beta}^2}{8},$$
$$\overline{R} = \frac{\overline{Q}}{2} \pm \sqrt{\frac{\overline{Q}^2}{4} + \frac{\overline{P}^3}{27}},$$
$$\overline{U} = \sqrt[3]{\overline{R}},$$
$$\overline{\xi} = -\frac{5\overline{\alpha}}{6} + \frac{\overline{P}}{3\overline{U}} - \overline{U}.$$

From (27), one can get

$$\overline{A}x_1^4 + \overline{B}x_1^3 + \overline{C}x_1^2 + \overline{D}x_1 + \overline{E} = 0. \tag{28}$$

If $\overline{\beta} = 0$ and $\overline{\alpha} < -2\sqrt{r}$, then the equation (28) has four real roots denoted as

$$\overline{x}_{11} = -\frac{\overline{B}}{4\overline{A}} + \sqrt{\frac{-\overline{\alpha} + \sqrt{\overline{\alpha}^2 - 4r}}{2}},$$

$$\overline{x}_{12} = -\frac{\overline{B}}{4\overline{A}} + \sqrt{\frac{-\overline{\alpha} - \sqrt{\overline{\alpha}^2 - 4r}}{2}},$$

$$\overline{x}_{13} = -\frac{\overline{B}}{4\overline{A}} - \sqrt{\frac{-\overline{\alpha} + \sqrt{\overline{\alpha}^2 - 4r}}{2}},$$

$$\overline{x}_{14} = -\frac{\overline{B}}{4\overline{A}} - \sqrt{\frac{-\overline{\alpha} - \sqrt{\overline{\alpha}^2 - 4r}}{2}}.$$

If $\overline{\beta} \neq 0$, $\overline{\alpha} + 2\overline{\xi} > 0$ and $3\overline{\alpha} + 2\overline{\xi} < \frac{2\overline{\beta}}{\sqrt{2\overline{\xi}+\overline{\alpha}}}$ or $3\overline{\alpha} + 2\overline{\xi} < -\frac{2\overline{\beta}}{\sqrt{2\overline{\xi}+\overline{\alpha}}}$, then equation (28) has real roots denoted as

$$\overline{x}'_{11} = -\frac{\overline{B}}{4\overline{A}} + \frac{-\sqrt{\overline{\alpha} + 2\overline{\xi}} \pm \sqrt{-(3\overline{\alpha} + 2\overline{\xi} - \frac{2\overline{\beta}}{\sqrt{\overline{\alpha}+2\overline{\xi}}})}}{2},$$

or

$$\overline{x}'_{11} = -\frac{\overline{B}}{4\overline{A}} + \frac{\sqrt{\overline{\alpha} + 2\overline{\xi}} \pm \sqrt{-(3\overline{\alpha} + 2\overline{\xi} + \frac{2\overline{\beta}}{\sqrt{\overline{\alpha}+2\overline{\xi}}})}}{2}.$$

By a simple calculation, we get

$$\begin{aligned} |DF^2(z_1)| =& 4\Big\{ -a^2y_1^2 + \Big[\Big(x_1 - \frac{1}{2}\Big)(x_1 - 2y_1)r + \frac{3}{2} - \frac{1}{2}x_1\Big]a - \frac{1}{2} + \Big(x_1 - \frac{1}{2}\Big)r\Big\} \\ &\times \big\{ -1 + (-2y_1^2 + 3x_1y_1)a^2 + \big[(x_1^2 - x_1)r + 2y_1 - x_1\big]a\big\} \\ &\times \Big[rax_1y_1 + \frac{1}{2} + (x_1^2 - x_1)r^2 + \Big(-x_1 + \frac{1}{2}\Big)r\Big]. \end{aligned}$$

Obviously, if the condition in Lemma 1 is satisfied and the solutions of Eqs. (25) and (27) satisfy that $z_1(x_1, y_1), z(x_2, y_2) \neq z_0(x_0, y_0), z_1(x_1, y_1) \in U_{z_0}$ and $|DF^2(z_1)| \neq 0$, then z_0 is a snap-back repeller in U_{z_0}. Thus, the following theorem is established.

Theorem 3. *Assume that the conditions in Lemma 1 hold. If*

(1) $-2ax_0 < r(1 - 2x_0) < 2ax_0$ *and* $(r - 2rx_0 - 2ax_0)(1 - ax_0) > 0$, *and*

(2) the solutions (x_2, y_2) *and* (x_1, y_1) *of Eqs. (25) and (27) satisfy that* (x_1, y_1), $(x_2, y_2) \neq (x_0, y_0)$, $(x_1, y_1) \in U_{z_0}$, $(x_1, y_1) \neq (0, 0)$ *and* $|DF^2(z_1)| \neq 0$.

Then $z_0(x_0, y_0)$ *is a snap-back repeller of map (1), and hence map (1) is chaotic in the sense of Marotto.*

Next, we give specific values of the parameters for illustrating the existence of conditions in Theorem 3.

Example 1. For $a = 1.5$ and $r = 4$, the map (1) has a fixed point $z_0(x_0, y_0) = (0.7272727273, 0.7272727273)$, and the eigenvalues associated with z_0 is $\lambda_{1,2} = -0.514234591 \pm 0.9544473351i$. Based on Lemma 1 and Theorem 3, we find that a region of z_0 is $U = \big\{(x, y) \mid 0.5 < x < 0.74,\ \overline{y_2}' < y < \overline{y_2}\big\} \subset U_{z_0} = \big\{(x,\ y) \mid x \in D_1,\ y \in D_3 \cup D_3'\big\}$, and there exists a

point $z_1(x_1,\ y_1) = (0.5110659317, 0.8236756974)$ satisfying that $F^2(z_1) = z_0$ and $|DF^2(z_1)| = -2.405093121 \neq 0$, where

$$\begin{aligned}\overline{y}_2 =&8.3333333x - 2.66666667 + 0.6666666667\sqrt{9x^2 - 6(4 - 9.5\ x)\ x},\\ \overline{y_2'} =&1.833333333 - 2.666666667x + 0.1111111111\\ &\times \sqrt{(16.5 - 24x)^2 - 72 + 144x - 18(7.5 - 12x)x}.\end{aligned}$$

Obviously $z_0, z_1 \in U$. Thus, z_0 is a snapback repeller.

Example 2. For $a = 1.55$ and $r = 4$, the map (1) has a fixed point $z_0(x_0, y_0) = (0.7207207, 0.7207207207)$, and the eigenvalues associated with z_0 is $\lambda_{1,2} = -0.4376068055 \pm 0.9307112097i$. Based on Lemma 1 and Theorem 3, we find that a region of z_0 is $U = \big\{(x, y) \mid 0.45 < x < 0.75,\ \overline{y_2}' < y < \overline{y_2}\big\} \subset U_{z_0} = \big\{(x,\ y) \mid x \in D_1,\ y \in D_3 \cup D_3'\big\}$, and there exists a point $z_1(x_1, y_1) = (0.4910895415, 0.7973518427)$ satisfying that $F^2(z_1) = z_0$ and $|DF^2(z_1)| = -2.346889713 \neq 0$, where

$$\begin{aligned}\overline{y}_2 =&8.161290322x - 2.580645161 + 6.451612903 \times \sqrt{9.61\ x^2 - 6.214\ (4 - 9.55\ x)\ x},\\ \overline{y_2'} =&1.774193548 - 2.58064516\ x + \ 0.1040582726\\ &\times \sqrt{(17.05 - 24.8xx)^2 - -76.88 + 153.76 - 19.22(7.55 - 12.4x)x}.\end{aligned}$$

Obviously $z_0,\ z_1 \in U$. Thus, z_0 is a snapback repeller.

5 Numerical Simulations

In this section, numerical simulations are given, including bifurcation diagrams, Lyapunov exponents (ML), fractal dimension (FD) and phase portraits, to illustrate the above theoretical analysis and show new and more complex dynamic behaviors in the map (1).

The fractal dimension [1, 12] is defined by using Lyapunov exponents as follows:

$$d_L = j + \frac{\sum\limits_{i=1}^{i=j} L_i}{L_j}$$

with $L_1, L_2, \cdots, L_n$, which are Lyapunov exponents, where j is the largest integer such that $\sum\limits_{i=1}^{i=j} \geq 0$ and $\sum\limits_{i=1}^{i=j+1} < 0$.

Our model is a two-dimensional map which has the fractal dimension

$$d_L = 1 + \frac{L_1}{|L_2|}, \qquad L_1 > 0 > L_2.$$

5.1 Numerical Simulations on Stability and Codimension One Bifurcations of Fixed Points

The following two cases are considered:

Case 1. Bifurcation diagram of map (1) in (a, x) plane for $0.2 \leq a \leq 1$, and $r = 2.9148$ with initial values $(0.75, 0.75)$ is given in Fig.1 (a), which shows that there are flip bifurcation (labeled "PD") emerging from the fixed point $z_0(0.7846, 0.7846)$ with $r = 2.9148$, $\alpha_1 = 4.11476532$ and $\alpha_2 = 84.39293744 > 0$.

Case 2. Bifurcation diagram of map (1) in (a, x) plane is given in Fig.1 (b) for $1.4 < a \leq 1.81$ and $r = 2.5$ with initial values $(0.75, 0.75)$. Fig.1 (b) exhibits Hopf bifurcation (labeled "HB"), which occurs at fixed point $z_0(0.6, 0.6)$ and $a = 1.6665$ with $d = 0.7500750075 > 0$, $l_1 = -4.417416610 < 0$. Fig.1 (a) and (b) verify the correctness of Theorem 1–2.

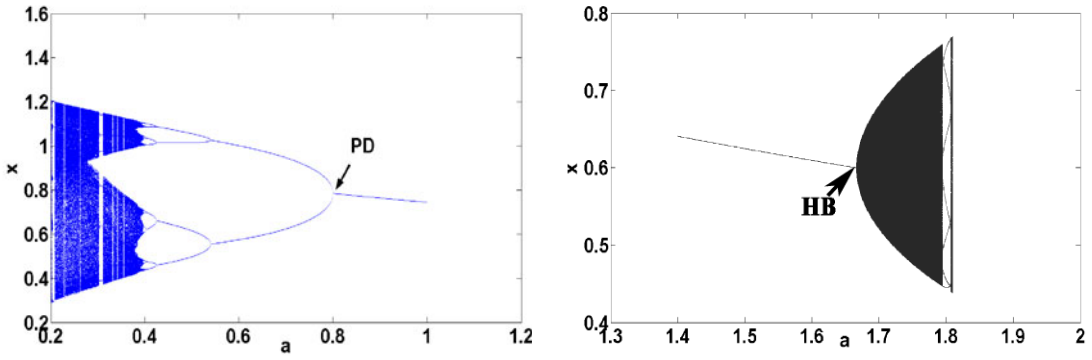

(a) (b)

Fig.1 (a) Bifurcation diagram of map (1) in (a, x)-plane for $r = 2.9148$ with $(x_0, y_0) = (0.75, 0.75)$.
(b) Bifurcation diagram of map (1) in (a, x)-plane for $r = 2.5$ with $(x_0, y_0) = (0.75, 0.75)$.

5.2 Numerical Simulations for Marotto's Chaos

In this subsection, numerical simulations are shown for verifying the condition in Theorem 3.

(1) By Example (1), the bifurcation diagram in (a, x) plane is given in Fig.2 (a) for $r = 4$ and $a \in (1.495, 1.505)$ with initial values $(0.75, 0.75)$. The maximum Lyapunov exponents corresponding to (a) are computed as shown in Fig.2 (b). From Example (1) and Theorem 3, one can see that the chaotic attractor is located in the chaotic region $a \in (1.499, 1.5005)$. In fact, for $a = 1.5$, $z_0(x_0, y_0) = (0.7272727273, 0.7272727273)$ is a fixed point of map (1), the region of z_0 is $U = \{(x,\ y) \mid 0.5 < x < 0.74,\ \overline{y_2}' < y < \overline{y_2}\} \subset U_{z_0} = \{(x,\ y) \mid x \in D_1,\ y \in D_3 \cup D_3'\}$ in which z_0 is expanding, and the point $z_1(x_1, y_1) = (0.5110659317, 0.8236756974)$ satisifes $F^2(z_1) = z_0$ and $|DF^2(z_1)| = -2.405093121 \neq 0$. Thus z_0 is a snapback repeller. The Marotto's chaotic attractor is given in Fig.2(c) for $u = 1.5$, which verifies Theorem 3.

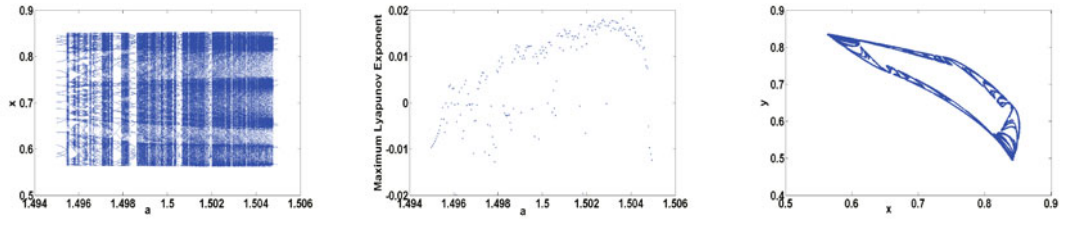

(a) (b) (c)

Fig.2 (a) Bifurcation diagram of map (1) in (a, x)-plane for $r = 4$ with $(x_0, y_0) = (0.75, 0.75)$.
(b) Maximum Lyapunov exponents corresponding to (a).
(c) Chaotic attractor $(ML = 0.0122, FD = 1.298)$ at $a = 1.5$ in (a).

(2) By Example (2), the bifurcation diagram in (a, x) plane is shown in Fig.3 (a) for $r = 4$ and $a \in (1.54,\ 1.558)$ with initial values $(0.75,\ 0.75)$, and the corresponding maximum Lyapunov exponents is given in Fig.3 (b). From Example (2) and Theorem 3, one can find that the chaotic attractor is located in the chaotic region $a \in (1.545,\ 1.551)$. In fact, for $a = 1.55$, $z_0(x_0,\ y_0) = (0.7207207207,\ 0.7207207207)$ is a fixed point of map (1), the region of z_0 is $U = \{(x, y) \mid 0.45 < x < 0.75,\ \overline{y_2}' < y < \overline{y_2}\} \subset U_{z_0} = \{(x,\ y) \mid x \in D_1,\ y \in D_3 \cup D_3'\}$ in which z_0 is expanding, and the point $z_1(x_1, y_1) = (0.4910895415, 0.7973518427)$ satisfies $F^2(z_1) = z_0$ and $|DF^2(z_1)| = -2.346889713 \neq 0$. Thus z_0 is a snapback repeller. The chaotic attractor is given in Fig.3(c) for $a = 1.55$, which is verifies Theorem 3.

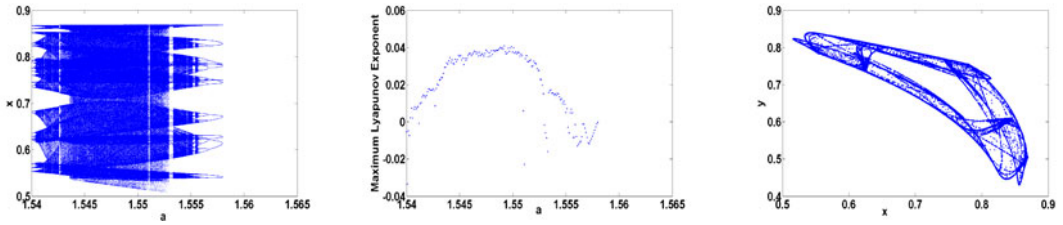

(a) (b) (c)

Fig.3 (a) Bifurcation diagram of map (1) in (a, x)-plane for $r = 4$ with $(x_0, y_0) = (0.75, 0.75)$.

(b) Maximum Lyapunov exponents corresponding to (a).

(c) Chaotic attractor ($ML = 0.03725,\ \ FD = 1.6085$) at $a = 1.55$ in (a).

5.3 Further Numerical Simulations for the Map (1)

In this subsection, new and complex dynamical behaviors are investigated as the parameters vary.

The bifurcation diagrams in the two-dimensional plane are considered in the following eight cases:

(ai) Varying a in range $0 \leq a \leq 1.857$ and fixing $r = 2.7$;
(aii) Varying a in range $0 \leq a \leq 1.724$ and fixing $r = 2.8$;
(aiii) Varying a in range $0 \leq a \leq 1.4985$ and fixing $r = 3$;
(aiv) Varying a in range $0.91 \leq a \leq 1.48$ and fixing $r = 3.5$;
(bi) Varying r in range $0.945 \leq r \leq 3$ and fixing $a = 1.5$;
(bii) Varying r in range $0 \leq r \leq 2.77$ and fixing $a = 1.9$;
(biii) Varying r in range $0.1 \leq r \leq 2.71$ and fixing $a = 2$;
(biv) Varying r in range $0 \leq r \leq 2.24$ and fixing $a = 2.1$.

For case (ai). The bifurcation diagram of map (1) in (a, x) plane is shown in Fig.4 (a) for $r = 2.7$ with initial values $(0.75,\ 0.75)$, and the maximum Lyapunov exponent corresponding to Fig.4 (a) is given in Fig.4 (b). In Fig.4, we observe that there are a stable fixed point for $a \in (0.642,\ 1.588)$, and a Hopf bifurcation occuring at $a \sim 1.588$, the simultaneous occurrence of two different routs (inverse period-doubling bifurcation and invariant circle) to chaos. One can also see that inverse period-doubling bifurcation, which occurs at $a \sim 0.642$, changes into chaos with interior crisis at $a \sim 0.0265$ and the chaotic behaviors suddenly appear at $a \sim 0$ and $a \sim 1.86$. Fig.4 (c)–(e) present the four-coexisting chaotic sets at $a = 0.13$, non-attracting chaotic sets at $a = 0.144$ and the invariant circle at $a = 1.6$, respectively.

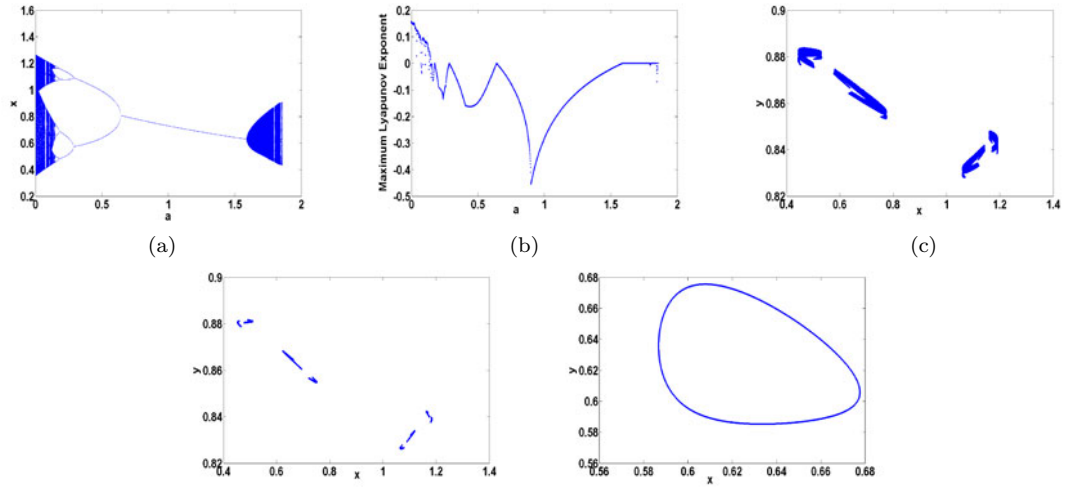

(a) (b) (c)

(d) (e)

Fig.4 (a) Bifurcation diagram of map (1) in (a, x)-plane for $r = 2.7$ and $0 \leq a \leq 1.857$ with $(x_0, y_0) = (0.75, 0.75)$.

(b) Maximum Lyapunov exponents corresponding to (a).

Phase portraits:

(c) four-coexisting chaotic sets ($ML = 0.051,\ FD = 1.9523$) for $a = 0.13$ in (a);

(d) non-attracting chaotic sets ($ML = 0.0225,\ FD = 1.4346$) for $a = 0.144$ in (a);

(e) invariant circle ($ML = 0$) for $a = 1.6$ in (a).

For case (aii). The bifurcation diagram of map (1) in (a, x) plane is shown in Fig.5 (a) for $r = 2.8$ with initial values $(0.77, 0.77)$, local amplification is given Fig.5 (b) and (c) for $a \in (0,\ 0.2)$ and $a \in (1.6, 1.7)$, and the maximum Lyapunov exponents corresponding to (a) is given in Fig.5 (d). One can observe that there are a stable fixed point for $a \in (0.718,\ 1.335)$, period-three orbits for $a \in [1.335, 1.488)$, and the simultaneous occurrence of two different routs (inverse period-doubling bifurcation and period-doubling bifurcation) to chaos. Moreover, there is a great abundance of period windows in the chaotic regions with interior crisis at $a \sim 0.0645$ and 0.14, and the chaotic behaviors suddenly appear at $a \sim 0$ and $a \sim 1.725$. Fig.5 (e)–(g) give the two-coexisting chaotic sets at $a = 0.22$, three-coexisting chaotic sets at $a = 1.7$, chaotic attractor at $a = 1.722$.

For case (aiii). The bifurcation diagram of map (1) in (a, x) plane is shown in Fig.6 (a) for $r = 3$ with initial values $(0.77,\ 0.77)$, are local amplification is given in Fig.6 (b) for $a \in (1.48,\ 1.4985)$, and the maximum Lyapunov exponent corresponding to (a) is given in Fig.6 (c). From the diagrams, One can observe that there is a period-one orbit region for $a \in (0.858,\ 1.48624)$, the fixed point loses its stability as a decreases and inverse period-doubling bifurcation which occurs at $a \sim 0.858$ changes into chaos with small complex period windows and the chaotic behavior suddenly appears at $a \sim 0$. Moreover, as a increases, the period-one orbit suddenly becomes period-14 orbits at $a \sim 1.48624$ and period-doubling bifurcation changes into chaos with period-one windows, and the chaotic behavior suddenly disappears at $a \sim 1.4986$. The nice chaotic attractors at $a = 1.498$ is shown in Fig.6 (d).

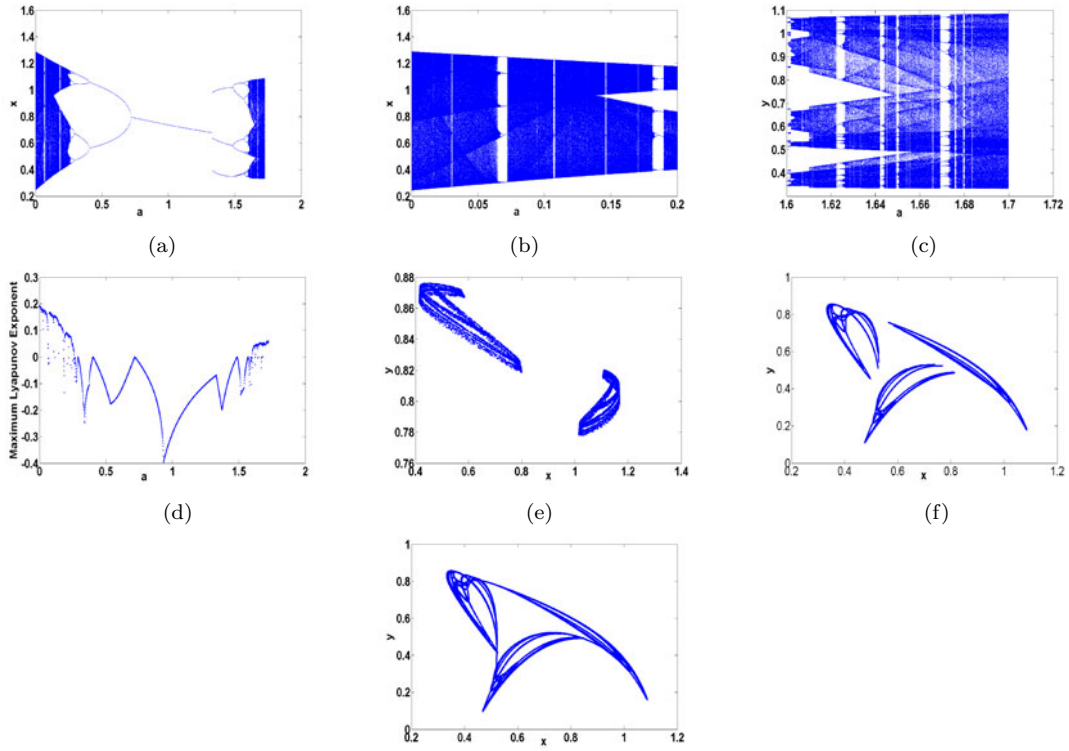

Fig.5 (a) Bifurcation diagrams of map (1) in (a, x)-plane for $r = 2.8$ and $0 \leq a \leq 1.724$ with $(x_0, y_0) = (0.77, 0.77)$.

(b) local amplification for $a \in (0,\ 0.2)$;

(c) Maximum Lyapunov exponents corresponding to (a).

(d) Maximum Lyapunov exponents corresponding to (a);

Phase portraits:

(e) the two coexisting chaotic sets ($ML = 0.05,\ FD = 1.5055$) for $a = 0.22$ in (a);

(f) three-coexisting chaotic sets ($ML = 0.0468,\ FD = 1.3824$) for $a = 1.7$ in (a);

(g) chaotic attractor ($ML = 0.05626,\ FD = 1.4899$) for $a = 1.722$ in (a).

For case (aiv). The bifurcation diagram of map (1) in (a, x) plane is shown in Fig.7 (a) for $r = 3.5$ with initial values $(0.77, 0.77)$, the maximum Lyapunov exponent corresponding to (a) is given in Fig.7 (b). The diagrams show that there are a period-one orbit region for $a \in (1.135,\ 1.4)$, the simultaneous occurrence of two different routs (inverse period-doubling bifurcation and invariant circle) to chaos with small period windows and interior crisis which occurs at $a \sim 0.999$. The chaotic attractor at $a = 0.92$ and two-coexisting chaotic sets at $a = 1$ are given in Fig.7 (c) and (d), respectively.

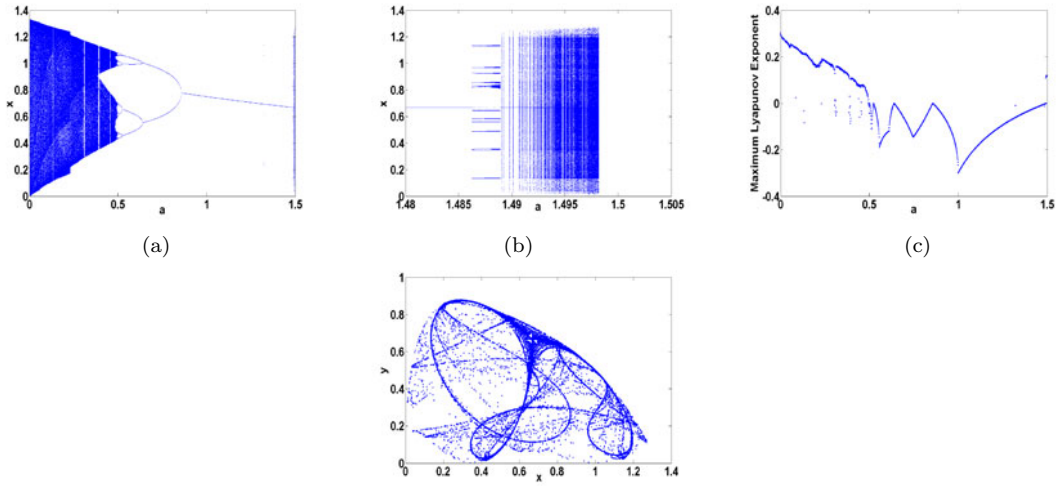

(a) (b) (c)

(d)

Fig.6 (a) Bifurcation diagrams of map (1) in (a, x)-plane for $r = 3$ and $0 \leq a \leq 1.4985$ with $(x_0, y_0) = (0.77, 0.77)$.

(b) The local amplification of (a) for $1.48 \leq a \leq 1.4985$.

(c) Maximum Lyapunov exponents corresponding to (a).

(d) Chaotic attractor ($ML = 0.1089,\ FD = 1.7559$) for $r = 1.498$ in (a).

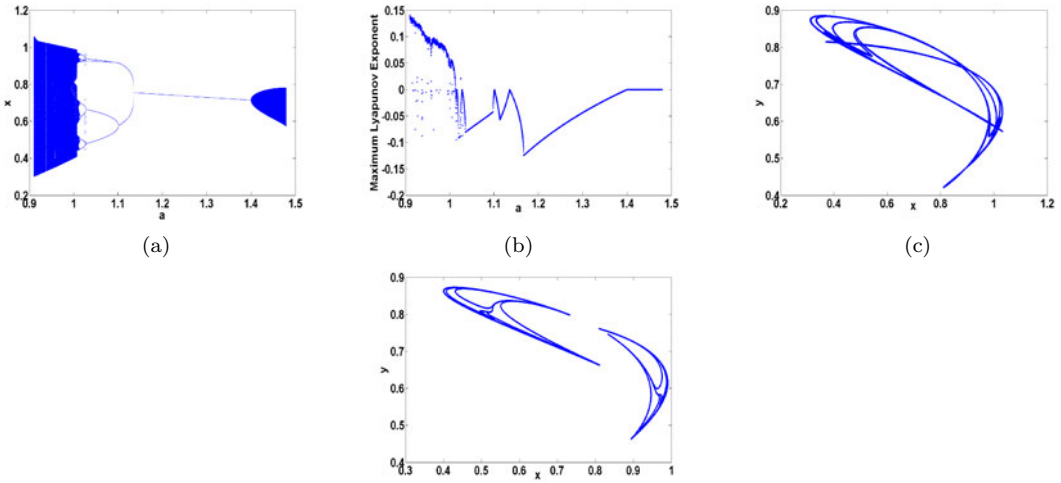

(a) (b) (c)

(d)

Fig.7 (a) Bifurcation diagram of map (1) in (a, x)-plane for $r = 3.5$ and $0.91 \leq a \leq 1.48$ with $(x_0, y_0) = (0.755, 0.755)$.

(b) Maximum Lyapunov exponents corresponding to (a).

Phase portraits:

(c) chaotic attractor ($ML = 0.13,\ FD = 1.2640$) for $a = 0.92$ in (a);

(d) two-coexisting chaotic sets ($ML = 0.05, FD = 1.1786$) for $a = 1$ in (a).

For case (bi). The bifurcation diagram of map (1) in (r, x) plane is shown in Fig.8 (a) for $a = 1.5$ with initial values $(0.75, 0.75)$, the maximum Lyapunov exponent corresponding to (a) is given in Fig.8 (b). From Fig.8 (a)–(b), one can see that there is a large stable region for $r \in (0.945,\ 2.72)$, period-one orbit becomes period-three orbits suddenly at $r \sim 2.72$ and period doubling bifurcation changes into chaos with period-one windows, and the chaotic behavior suddenly disappears at $r \sim 3$. The three-coexisting chaotic sets at $r = 2.9321$, chaotic attractor at $r = 2.998$ are exhibited in Fig.8 (c)-(d), respectively.

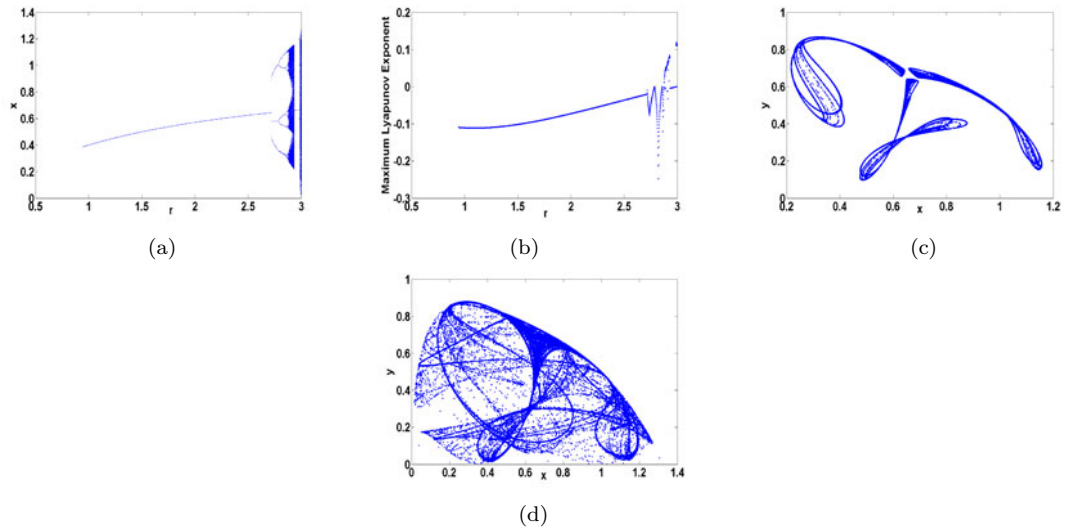

(a) (b) (c)

(d)

Fig.8 (a) Bifurcation diagram of map (1) in (r, x)-plane for $a = 1.5$ and $0.945 \le r \le 3$ with $(x_0, y_0) = (0.75, 0.75)$.

(b) Maximum Lyapunov exponents corresponding to (a).

Phase portraits:

(c) three-coexisting chaotic sets ($ML = 0.08,\ FD = 1.4043$) for $r = 2.9321$ in (a);

(d) chaotic attractor ($ML = 0.1176, FD = 1.7576$) for $r = 2.998$ in (a).

For case (bii). The bifurcation diagram of map (1) in (r, x) plane is shown in Fig.9 (a) for $a = 1.9$ with initial values $(0.1, 0.1)$, Fig.9 (b) is the local amplification for $r \in (2.5,\ 2.77)$ in (a). The maximum Lyapunov exponent corresponding to (a) is given in Fig.9 (c). The diagrams show that there are a wider period-one orbit region for $r \in (0,\ 2.11)$ and sudden appearance of invariant circle as r increases and that the invariant circle suddenly becomes to period-7 orbits, the onset of chaos at $r \sim 2.6507$, and complex period windows in the chaotic region, and the chaotic behavior suddenly disappears at $r \sim 2.771$. The period chaos at $r = 2.652$ and period windows at $r = 2.69$ are plotted in Fig.9 (d) and (e), respectively.

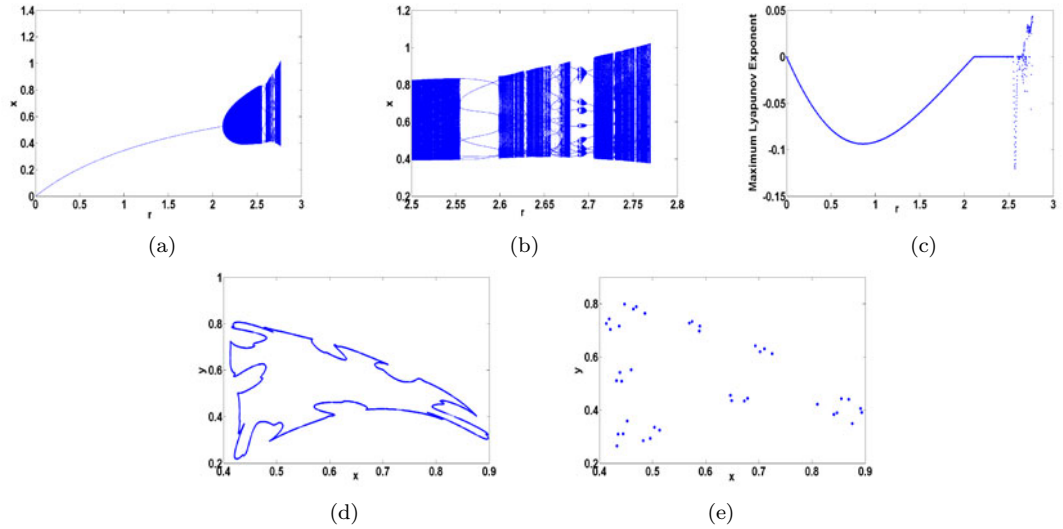

(a) (b) (c)

(d) (e)

Fig.9 (a) Bifurcation diagram of map (1) in (r, x)-plane for $a = 1.9$ and $0 \leq r \leq 2.77$ with $(x_0, y_0) = (0.1, 0.1)$.

(b) The local amplification of (a) for $2.5 \leq a \leq 2.77$.

(c) Maximum Lyapunov exponents corresponding to (a).

Phase portraits:

(d) (d) chaos ($ML = 0.0074,\ FD = 1.0312$) for $r = 2.652$ in (a);

(e) period window for $r = 2.69$ in (a).

For case (biii). The bifurcation diagram of map (1) in (r, x) plane for $a = 2$ with initial values $(0.51, 0.51)$ is shown in Fig.10 (a), and the maximum Lyapunov exponent corresponding to (a) is given in Fig.10 (b). The diagrams show that there is a period-one orbit region for $r \in (0.1,\ 2)$, the fixed point loses its stability as r increases, period-one orbit to period-4 orbits, which occurs at $r \sim 2$, changes into chaos with complex period windows, and the chaotic behavior suddenly disappears at $r \sim 2.711$. The four-coexisting chaotic sets at $r = 2.25$, chaotic attractor at $r = 2.4$ are exhibited in Fig.10 (c)–(d), respectively.

For case (biv). The bifurcation diagram of map (1) in (r, x) plane for $a = 2.1$ with initial values $(0.1, 0.1)$ is shown in Fig.11 (a) and the maximum Lyapunov exponent corresponding to (a) is given in Fig.11 (b). One can see that there is a stable fixed point for $r \in (0,\ 1.91)$, the fixed point loses its stability as r increases, the sudden appearance of invariant circle occurs at $r \sim 1.91$, the invariant circle suddenly becomes chaos at $r \sim 2.069$ with complex period windows, and the chaotic behavior suddenly disappears at $r \sim 2.241$. The non-attracting chaos at $r = 2.091$, chaotic attractor at $r = 2.109$, period orbits at $r = 2.13$, chaotic attractor at $r = 2.225$ are shown in Fig.11 (c)–(f), respectively.

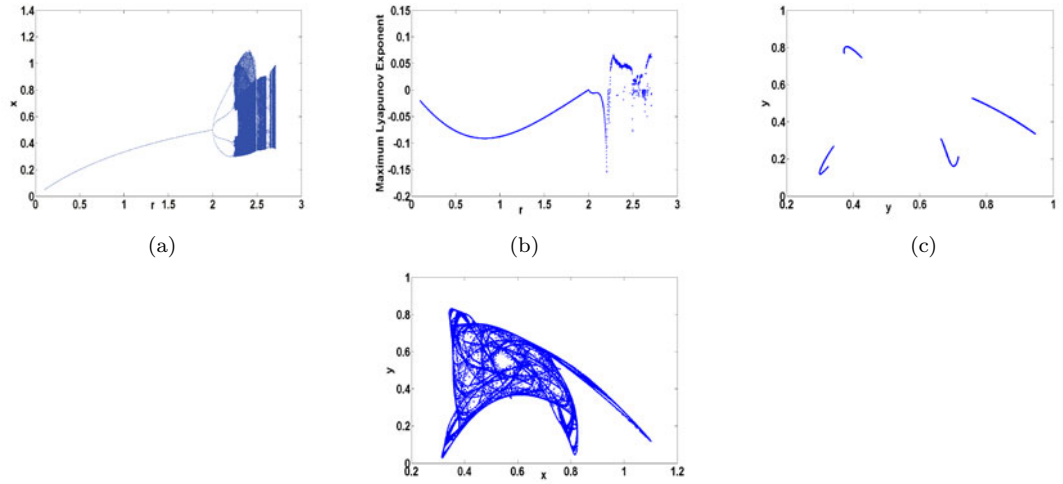

(a) (b) (c)

(d)

Fig.10 (a) Bifurcation diagram of map (1) in (r, x)-plane for $a = 2$ and $0.1 \leq r \leq 2.71$ with $(x_0, y_0) = (0.51, 0.51)$.

(b) Maximum Lyapunov exponents corresponding to (a).

Phase portraits:

(c) four-coexisting chaotic sets $(ML = 0.0433, FD = 1.1666)$ for $r = 2.25$ in (a);

(d) chaotic attractor $(ML = 0.0457, FD = 1.6160)$ for $r = 2.4$ in (a).

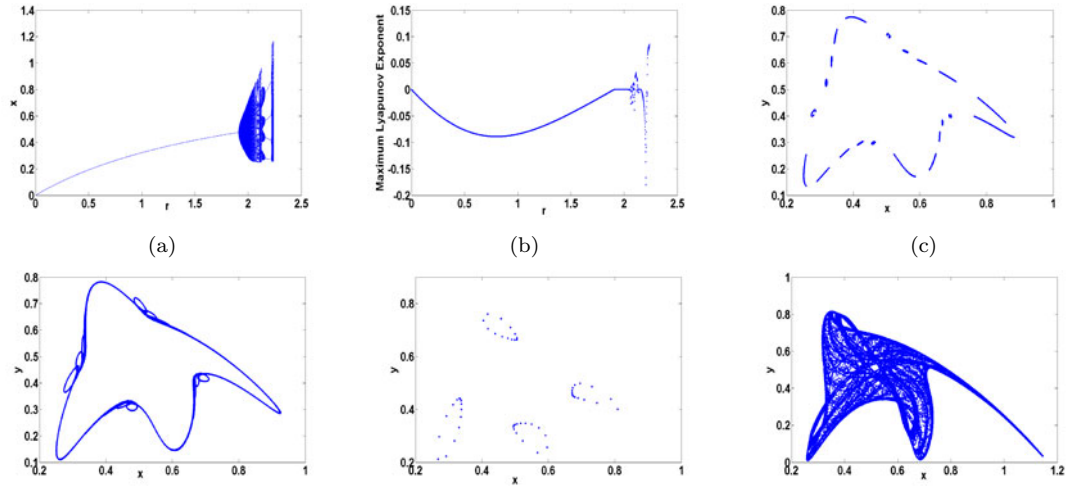

(a) (b) (c)

(d) (e) (f)

Fig.11 (a) Bifurcation diagram of map (1) in (r, x)-plane for $a = 2.1$ and $0 \leq r \leq 2.24$ with $(x_0, y_0) = (0.1, 0.1)$.

(b) Maximum Lyapunov exponents corresponding to (a).

Phase portraits:

(c) non-attracting chaos $(ML = 0.012,\ FD = 1.1471)$ for $r = 2.091$ in (a);

(d) chaotic attractor $(ML = 0.0283,\ FD = 1.4104)$ for $r = 2.109$ in (a);

(e) period orbits $(ML = -0.00025)$ for $r = 2.13$ in (a);

(f) chaotic attractor $(ML = 0.071,\ FD = 1.8461)$ for $r = 2.225$ in (a).

References

[1] Cartwright, J.H.E. Nonlinear stiffness, Lyapunov exponents, and attractor dimension. *Phys. Lett. A.*, 264: 298–302 (1999)

[2] Celik, C., Duman, O. Allee effect in a discrete-time predator-prey system. *Chaos, Solitons and Fractal*, 40: 1956–1962 (2009)

[3] Chen, X.W., Fu, X.L, Jing, Z.J. Dynamics in a Discrete-time Predator-prey System with Allee Effect. *Acta Mathematicae Applicatae Sinica*, 29: 143–164 (2012)

[4] Cheng, Z., Lin, Y., Cao, J. Dynamical behaviors of a partial-dependent predator-prey system. *Chaos, Solitons and Fractals*, 28: 67–75 (2006)

[5] Chen, X. Periodicity in a nonlinear discrete predator-prey system with state dependent delays. *Nonlinear Anal RWA.*, 8: 435-446 (2007)

[6] Choudhury, S.R. On bifurcations and chaos in predator-prey models with delay. *Chaos, Solitons and Fractals*, 2: 393–409 (1992)

[7] Fan, M., Agarwal, S. Periodic solutions of nonautonomous discrete predator-prey system of Lotka-Volterra type. *Appl Anal.*, 81: 801–812 (2002)

[8] Guckenheimer, J., Holmes, P. Nonlinear oscillations, dynamical systems and bifurcations of vector fields. New York: Springer-Verlag, 1983

[9] Jiang, G., Lu, Q. Impulsive state feedback of a predator-prey model. *J. Comput. Appl. Math.*, 200: 193–207 (2007)

[10] Jiang, G., Lu, Q., Qian, L. Complex dynamics of a Hollingtype II prey-predator system with state feedback control. *Chaos, Solitons and Fractals*, 31: 448–461 (2007)

[11] Jing, Z.J, Yang, J.P. Bifurcation and chaos in discrete-time predator-prey system. *Chaos, Solitons and Fractals*, 27: 259–277 (2006)

[12] Kaplan, J.L., Yorke, J.A. Aregime observed in a fluid flow model of Lorenz. *Comm. Math. Phys.*, 67: 93–108 (1979)

[13] Kendall, B.E. Cycles, chaos, and noise in predator-prey dynamics. *Chaos, Solitons and Fractals*, 12: 321–332 (2001)

[14] Liu, B., Teng, Z., Chen, L. Analysis of a predator-prey model with Holling II functional response concerning impulsive control strategy. *J. Comput. Appl. Math.*, 193: 347–362 (2006)

[15] Liu, X., Xiao, D. Complex dynamic behaviors of a discrete-time predator-prey system. *Chaos, Solitons and Fractals*, 32: 80–94 (2007)

[16] Marotto, F.R. On redefining a snap-back repeller. *Chaos, Solitons and Fractals*, 25: 25–28 (2005)

[17] Marotto, F.R. Snap-back repellers imply chaos in R_n. *J. Math. Anal. Appl.*, 63: 199–223 (1978)

[18] Ma, W., Takeuchi, Y. Stability analysis on a predator-prey system with distributed delays. *J. Comput. Appl. Math.*, 88: 79–94 (1998)

[19] Moghadas, S.M., Corbett, B.D. Limit cycles in a generalized Gause-type predator-prey model. *Chaos, Solitons and Fractals*, 37(5): 1343–1355 (2008)

[20] Sun, C., Han, M., Lin, Y., Chen, Y. Global qualitative analysis for a predator-prey system with delay. *Chaos, Solitons and Fractals*, 32: 1582–1596 (2007)

[21] Teng Z, Rehim M. Persistence in nonautonomous predator-prey systems with infinite delays. *J. Comput. Appl. Math.*, 197: 302–321 (2006)

[22] Wang, F., Zeng, G. Chaos in Lotka-Volterra predator-prey system with periodically impulsive ratio-harvesting the prey and time delays. *Chaos, Solitons and Fractals*, 32: 1499–1512 (2007)

[23] Wang, L.L, Li, W.T, Zhao, P.H. Existence and global stability of positive periodic solutions of a discrete predator-prey system with delays. *Adv Differen Equat.*, 4: 321–336 (2004)

[24] Wiggins, S. Introduction to applied nonlinear dynamical systems and chaos. Berlin: Springer-Verlag, 1990

[25] Xiao, Y., Cheng, D., Tang, S. Dynamic complexities in predator-prey ecosystem models with age-structure for predator. *Chaos, Solitons and Fractals*, 14: 1403–1411 (2002)

[26] Xu, R., Wang, Z. Periodic solutions of a nonautonomous predator-prey system with stage structure and time delays. *J. Comput. Appl. Math.*, 196: 70–86 (2006)

[27] Yan, X.P, Chu, Y.D. Stability and bifurcation analysis for a delayed Lotka-Volterra predator-prey system. *J. Comput. Appl. Math.*, 196: 198–210 (2006)